Pure Appl. Geophys. 177 (2020), 1005–1027

https://doi.org/10.1007/s00024-019-02306-0

Pure and Applied Geophysics

3-D Gravity Anomaly Inversion Based on Improved Guided Fuzzy *C*-Means Clustering Algorithm

Sheng Liu[1,2,3] and Shuanggen Jin[3,4]

Abstract—The geophysical inversion with combining prior information is very important for resource exploration and studies of the Earth's internal structure. Guided fuzzy *C*-means clustering inversion (FCM) is normally applied for the Tikhonov regularized inversion, but has the shortcoming of uniform model parameter shrinkage, leading to inaccuracy. In this paper, an improved guided fuzzy clustering algorithm is proposed by adding a fuzzy entropy term to the original guided FCM. This method not only enforces the discrete values to a high degree of approximation by guiding the recovered model to cluster tightly around the known petrophysical property values, but also calculates the distributed characteristics of the model parameter set. Based on this method, the shortcoming of uniform shrinkage of the original guided FCM clustering algorithm is improved, and more accurate inversion results are obtained, making the FCM method more efficient and broadly applicable. Furthermore, a new parameter search algorithm is proposed to accelerate the search speed. The results recovered by using this method with three kinds of theoretical gravity anomaly data show more accurate density anomalies compared with the results generated from the original guided FCM clustering inversion and greater efficiency in the parametric search process when using the new parameter search algorithm. The improved FCM clustering algorithm could enable more extensive and efficient use of gravity inversion.

Key words: Fuzzy entropy, discrete-valued inversion, gravity inversion, parameter search, fuzzy *C*-means algorithm.

[1] Xinjiang Astronomical Observatory, Chinese Academy of Sciences, Urumqi 830011, China.
[2] University of Chinese Academy of Sciences, Beijing 100049, China.
[3] Shanghai Astronomical Observatory, Chinese Academy of Sciences, Shanghai 200030, China. E-mail: sgjin@shao.ac.cn; sg.jin@yahoo.com
[4] School of Remote Sensing and Geomatics Engineering, Nanjing University of Information Science and Technology, Nanjing 210044, China.

1. Introduction

Three-dimensional (3-D) petrophysical inversion has been widely used in resource exploration and studies of the Earth's internal structure. The general approach is to find the minimum of an objective function based on the L_2-norm, resulting in a model whose petrophysical property values typically vary smoothly across the volume of interest (e.g., Constable et al. 1987; de Groot-Hedlin and Constable 1990; Holtham and Oldenburg 2012; Li and Oldenburg 1996, 1998, 2000, 2003; Mackie and Madden 1993; Newman and Alumbaugh 2000; Sun and Li 2010; Zelt and Barton 1998). However, the boundaries between geological units are not clear, and the inverted petrophysical property values exhibit less variability than the true values (Lelièvre and Oldenburg 2009). Several types of prior information can be used to improve the recovered model in such petrophysical inversion (e.g., Farquharson et al. 2008; Lane et al. 2007). Indeed, multiple categories of priori information can be incorporated into such inversions, including but not limited to petrophysical property measurements, structural orientations, geostatistical information, and the expected shape of a target (Farquharson et al. 2008; Lelièvre and Oldenburg 2009; Phillips 2001; Williams 2008).

One key issue is how to use petrophysical information in a regularized inversion based on the L_2-norm. Several methods are currently used for discrete inversion of gravity data. Krahenbuhl and Li (2006, 2009) solved the minimization in a regularized inversion via "binary inversion." Camacho et al. (2000) proposed a method of "growing bodies," which starts with an initial guess then increases the volume of the anomalous density body until a suitable solution is obtained. Uieda and Barbosa (2011) began with user-defined "seeds," each with a given density contrast. The seeded regions are then allowed to expand and form compact source bodies with varying density contrasts.

Although the aforementioned methods have wide applications for the inversion of field data, several problems remain. By restricting the model to have only two discrete values, one for the background geological body and the other for the target body, the minimization of the objective function becomes a quadratic integer programming problem. However, the calculation of this formula requires large amounts of computer memory and central processing unit (CPU) time (e.g., Chaovalitwongse et al. 2008).

There are also practical problems regarding the strict imposition of discrete values when using these methods. For instance, priori information of the density contrasts always has uncertainties, which will lead to imprecise inversion results. Elizabeth and Li (2018) proposed a method to approximate a discrete-valued inversion problem by applying the guided FCM clustering technique, which avoids the above computing challenges. This method enforces the recovered model to cluster tightly around the known petrophysical property values. The guided FCM clustering technique was initially proposed by Sun and Li (2015) and then applied by Sun and Li (2016) and Li and Sun (2016). This technique adds a "guiding" term to encourage the model parameters to cluster around the known petrophysical information.

Although these studies using the guided FCM clustering method solved several of the problems faced by classical methods, some problems still remain. The FCM clustering algorithm is a type of division method (Li et al. 2003), inevitably suffering from the disadvantage of uniform shrinkage of the clustering result of the model values during the convergence process (Li et al. 2004; Lin et al. 2009). This not only leads to the requirement for a lot of computing time and resources, but also limits the application of the method for petrophysical inversion. Therefore, it is important to overcome this shortcoming of uniform shrinkage with the FCM algorithm and to improve the clustering accuracy. The purpose of this paper is to address the above-mentioned shortcomings by combining the improved fuzzy *C*-means clustering algorithm (Xing et al. 2010) with the original guided FCM clustering method and to obtain a new algorithm for discrete-valued inversion.

FCM inversion relies heavily on the selection of the weighting parameters (Sun and Li 2015, 2016; Maag and Li 2018). In previous inversion algorithms, the parameters are manually adjusted during the inversion process (Sun and Li 2015, 2016). Maag and Li (2018) proposed an inversion workflow in which an enumeration method is used to select the optimal values of the weighting parameters. However, such methods undoubtedly increase the amount of calculations as well as the complexity of parameter selection. Thus, a new parameter selection algorithm based on a new FCM inversion method is proposed herein for the automatic selection of two weighting parameters in the FCM term to reduce the computational cost and the complexity of the selection process.

In the following, this improved FCM clustering technique based on regularization inversion is presented and discussed. Three-dimensional petrophysical inversion of gravity anomalies with two types of discrete density differences is then carried out to prove the correctness and advantages of the improved algorithm. Furthermore, the algorithm is validated using theoretical gravity anomaly data. Finally, some improved results for discrete-valued gravity inversion are presented and analyzed using the improved guided FCM clustering technique.

2. *Methodology*

We focus on the application of discrete petrophysical property values within an inversion by minimizing the objective function:

$$\min\Phi = \Phi_{\mathrm{d}} + \beta\Phi_{\mathrm{m}}, \tag{1}$$

$$\text{subject to}\, m_j \in \{0, 1\},$$

where Φ_{d} denotes the data misfit, Φ_{m} denotes the model objective function, and β denotes the

Tikhonov regularization parameter, subject to model parameters m_j with one of two discrete values. In some cases, when the densities of the anomalous body and the surrounding background rock are relatively uniform, it can be considered that there are two types of geological bodies in the area under consideration. However, after calculating the residual gravity anomaly from Bouguer gravity anomaly data, the density of the anomalous body becomes the difference between the original density value and the density value of the background geological body, while the density of the background geological body becomes 0 g/cc. For example, constant density values of 0 g/cc for the background and 1 g/cc for the anomalous region are used (Maag and Li 2018).

The guided FCM clustering was combined with Tikhonov regularized inversion by Sun and Li (2015) to include scattered petrophysical information. In practical applications, the clustering algorithm suffers from the disadvantage of uniform shrinkage, which causes inaccuracy. However, when considering the distribution characteristics of model parameter values during the inversion process, the inversion results will be more accurate. This section presents the inversion of the guided FCM clustering formulation with fuzzy entropy added to the regularization inversion formula, and then discusses how to minimize it.

2.1. Improved Guided Fuzzy Clustering Inversion

The inversion minimizes the following objective function using the guided FCM clustering algorithm presented by Sun and Li (2015):

$$\Phi(m,u,v) = \Phi_{\mathrm{d}} + \beta\Phi_{\mathrm{m}} + \lambda\Phi_{\mathrm{FCM}}, \tag{2}$$

which includes the data misfit (Φ_{d}), regularized parameter (β), model objective function (Φ_{m}), a weighting parameter for the clustering (λ), and the guided FCM clustering objective function (Φ_{FCM}).

Each component of the above objective function plays a different and significant role. Firstly consider the data misfit as:

$$\Phi_{\mathrm{d}} = \left\| W_{\mathrm{d}}(d_{\mathrm{pre}} - d_{\mathrm{obs}}) \right\|_2^2, \tag{3}$$

$d_{\mathrm{pre}} = Gm$,which computes the distance between the observed (d_{obs}) and predicted data (d_{pre}), multiplied by the data weighting matrix (W_d), which is a diagonal matrix with the inverse of the standard deviations of the data as its elements (Parker 1994; Aster et al. 2016).

A commonly used model structure term Φ_{m} has the following form (Li and Oldenburg 1996; Aster et al. 2016):

$$\Phi_{\mathrm{m}} = \| W_{\mathrm{m}}(m - m_{\mathrm{ref}}) \|_2^2, \tag{4}$$

$$W_{\mathrm{m}} = DS,$$

which measures the distance between the current model (m) and a reference model (m_{ref}), multiplied by the model weighting matrix (W_{m}). The model weighting matrix is defined as the discretized operator matrix (D) multiplied by a depth weighting matrix (S) chosen to counteract the natural decay with distance of the gravity kernel matrix (G). We choose to include a model objective function to encourage the spatial coherence of the recovered model.

The concrete form of the original guided FCM objective function can be expressed in the following specific form (Sun and Li 2015, 2016; Li and Sun 2016; Maag and Li 2018):

$$\Phi_{\mathrm{FCM}}(m,u,v) = \sum_{j=1}^{M}\sum_{k=1}^{C} u_{jk}^{q} \left\| m_j - v_k \right\|_2^2 + \eta\sum_{k=1}^{C} \| v_k - t_k \|_2^2, \tag{5}$$

where M is the number of model cells, u_{jk} measures the degree of the jth model cell belonging to the kth cluster, q is the fuzziness factor, C is the number of cluster categories, η is a scalar weighting parameter, the v_k are the cluster centers, and the t_k are the target cluster centers. In this paper, we choose q equal to 2.0 and a total number of clusters C as 2. The value of the membership function is greater than zero and less than one, and the sum of membership function values belonging to each class of each model is one:

$$\sum_{k=1}^{C} u_{jk} = 1. \tag{6}$$

In Eq. 5, given a number of objects such as petrophysical property values, the task of classifying them into a certain number of groups derived from prior petrophysical information can be accomplished by FCM clustering through minimization. However, the FCM clustering algorithm is a partitioning method and suffers from the disadvantage of a uniform shrinking trend of the clustering result. This not only consumes a lot of time and resources, but also limits the application of the FCM clustering algorithm for petrophysical inversion.

A more orderly system corresponds to lower information entropy (Zhang and Leung 2004). When the information entropy is introduced into the objective function of the FCM algorithm, the membership function of the sample points conforms to a Gaussian distribution, thereby effectively suppressing the influence of noise data on the cluster centers. To a certain extent, the use of the information entropy can thus make up for the shortcomings of the FCM algorithm (Xing et al. 2010). The fuzzy entropy can be defined by the following function:

$$E(x) = -\sum_{j=1}^{M}\sum_{k=1}^{C} u_{jk}^{q} \ln u_{jk}^{q}. \tag{7}$$

Adding this function for the fuzzy entropy term to the guided FCM clustering algorithm results in

$$\Phi_{\mathrm{EFCM}} = \sum_{j=1}^{M}\sum_{k=1}^{C} u_{jk}^{q} \left\| m_j - v_k \right\|_2^2 - \sum_{j=1}^{M}\sum_{k=1}^{C} \gamma_j u_{jk}^{q} \ln u_{jk}^{q} + \eta \sum_{k=1}^{C} \left\| v_k - t_k \right\|_2^2. \tag{8}$$

In Eq. 8, the second term estimates the distribution of petrophysical parameter data and a lower value of the fuzzy entropy indicates more ordered parameter values. The parameter γ is the fuzzy entropy parameter, whose specific form is mentioned in the next section.

The data misfit (Eq. 3), model objective function (Eq. 4), and improved FCM clustering objective function (Eq. 8) can be combined to obtain

$$\Phi(m, u, v) = \Phi_{\mathrm{d}} + \beta\Phi_{\mathrm{m}} + \lambda\Phi_{\mathrm{EFCM}}. \tag{9}$$

From Eq. 9, a model that fits the data, is spatially cohesive, and whose density values are well clustered to the target cluster values can be recovered. Additionally, by adding the fuzzy entropy term, a more accurate solution will be obtained.

2.2. *Minimization Algorithm for Improved Guided FCM Clustering*

To minimize the objective function in Eq. 9 with respect to these parameters, we choose a sequential minimization process. Provided that the final solution depends on the choice of these weighted parameters, the issue of determining those values will be fully considered.

2.2.1 *Sequential Minimization*

The improved guided FCM clustering technique requires the solutions for the petrophysical property model (m), cluster centers (v), and membership function (u). To minimize the objective function (Eq. 9) with respect to these variables, we use a sequential minimization process, and the details can be found in Maag and Li 2018, while herein we highlight the changes in the improved FCM clustering technique.

Firstly, to minimize the objective function in the direction of the membership values, we take the derivative of the objective function (Eq. 9) with respect to the u_{jk}. The result is then set to zero and solved for u_{jk}, resulting in

$$u_{jk} = \mathrm{e}^{\frac{\left\| m_j - v_k \right\|_2^2}{q\lambda_j} - \frac{1}{q}}. \tag{10}$$

Applying the result of Eqs. 6–10 yields the following formula for γ (Xing et al. 2010):

$$\gamma_j = \frac{1}{\sum_{i=1}^{C} \left\| m_j - v_i \right\|_2^2}. \tag{11}$$

Application of Eqs. 10 and 11 in Eq. 8 yields (Xing et al. 2010):

$$\Phi_{\mathrm{FCM}} = \sum_{j=1}^{M}\sum_{k=1}^{C} \frac{u_{jk}^{q}}{\sum_{i=1}^{C} \left\| m_j - v_i \right\|_2^2} + \eta \sum_{k=1}^{C} \left\| v_k - t_k \right\|_2^2. \tag{12}$$

We analyze the petrophysical meaning of $\frac{1}{\sum_{i=1}^{C} \left\| m_j - v_i \right\|_2^2}$, which actually represents a spatial distribution feature of petrophysical parameter data.

For convenience of expression and calculation, we set $\frac{1}{\sum_{i=1}^{C} \left\| m_j - v_i \right\|_2^2}$ equal to δ_j.

According to the above analysis, the original FCM (Eq. 5) algorithm is adjusted to obtain the formula as

$$\Phi(u,v,m) = \Phi_d(m) + \beta\Phi_m(m) + \lambda\left(\sum_{j=1}^{M}\sum_{k=1}^{C}\delta_j^q u_{jk}^q\left\|m_j - v_k\right\|_2^2 + \eta\sum_{k=1}^{C}\|v_k - t_k\|_2^2\right). \quad (13)$$

To minimize the objective function in the direction of the cluster centers, we take the derivative of the objective function (Eq. 13) with respect to the cluster centers v_k. The result is then set to zero and solved for v_k, resulting in

$$v_k = \frac{\sum_{j=1}^{M}\delta_j^q u_{jk}^q m_j + \eta t_k}{\sum_{j=1}^{M}\delta_j^q u_{jk}^q + \eta}. \quad (14)$$

We then take the derivative of the objective function (Eq. 13) with respect to the membership function values u_{jk}. The result is then set to zero and solved for u_{jk}, yielding:

$$u_{jk} = \left(\frac{\alpha_j}{q\delta_j^q\left\|m_j - v_k\right\|_2^2}\right)^{\frac{1}{q-1}}. \quad (15)$$

The following formula is then obtain after substituting Eq. 6 into Eq. 15:

$$\alpha^{\frac{1}{q-1}} = \sum_{k=1}^{C}\left(q\delta_j^q\left\|m_j - v_k\right\|_2^2\right)^{\frac{1}{q-1}}. \quad (16)$$

Substituting Eq. 16 into Eq. 15 yields:

$$u_{jk} = \frac{\left\|m_j - v_k\right\|^{\frac{-2}{q-1}}}{\sum_{i=1}^{C}\left\|m_j - v_i\right\|^{\frac{-2}{q-1}}}. \quad (17)$$

Thus, we derive the membership functions (Eq. 17) and cluster centers (Eq. 14) using the improved FCM algorithm. The membership function in this paper has the same form as proposed by Maag and Li (2018), but the cluster center formulas have a different form. Obviously, the newly proposed cluster center formula fully considers the data distribution of the petrophysical property model in the calculation, so that the calculation of the cluster centers can more reasonably represent the actual data.

2.3. *Inversion Workflow*

The value of β is determined based on the uncertainty in the data by methods such as the discrepancy principle (Parker 1994), which declare that the optimal value of β is that which can yield the expected value of the data misfit.

The prior model from the regularized inversion specifies an underground spatial distribution of a petrophysical property, and a similar spatial distribution for the subsequent inversion result. In this section, the variance of each cluster is used to estimate the quality of the recovered model defined as (Maag and Li 2018):

$$S_k = \sum_{i=1}^{M_k}\|m_i - t_k\|_2^2, \quad (18)$$

where m_i is the petrophysical property value belonging to the kth cluster which has the corresponding target petrophysical property value of t_k, and M_k is the number of model parameters in this cluster. We then assign model parameter values to each cluster, determined by their maximum membership value. Obviously, when the calculated variance values are smaller, the inverted petrophysical parameter model is better clustered around the discrete values, $\mathrm{t_k}$, the prior property information. Therefore, in the subsequent inversion process, our goal is to seek a model that produces tiny variance errors for each cluster and with data misfit close to the expected target data misfit.

To determine the optimal values of β, λ, and η, we use a workflow similar to that proposed by Maag and Li (2018). The inversion workflow and details are shown as follows:

1. Set the value of λ to zero and determine the value of β using the L-curve method. Then, perform a smooth inversion using the value of β, and take the obtained petrophysical property model as a reference model.
2. Carry out many inversions using many $\lambda - \eta$ pairs to obtain an optimal set of $\lambda - \eta$ values depending on the value of β and the reference model produced in the first step, as detailed in Algorithm 1. In each inversion, the data misfit (Eq. 3) and the variance of each cluster (Eq. 18) are recorded. Each of these

values is then drawn as a function of λ and η on logarithmic scales. Finally, the pair $\lambda - \eta$ that produces tiny variance values for each cluster and a data misfit close to the expected target data misfit is taken.

Algorithm 1 Algorithm for selection of the optimize values of λ and η

Compute reference model vector, m_{ref}, from smooth inversion based on regularization parameter, β from L-curve method. Assign termination tolerance value ε (a smaller positive constant, 5E-2). Initialize the initial clustering center v_k $(k=1,2)$. Based on petrophysical data, determine the target values, t_k $(k=1,2)$. Initialize the set of parameter pairs for λ and η, in this paper, the parameters of λ and η range from 1 to 10000. Initialize the value of iteration number $C1$(6). The number of iterations should not be too much, just to select the initial parameter values. Even if the number of iterations is large, the parameters are not properly selected, which consumes a lot of CPU calculation time and occupies a large amount of storage space.

step 1: Select a pair of parameters in the parameter pair sets of λ and η in order.

Set i=0 and n=0. Initialize $\delta^{(0)}$ ($\delta^{(0)} \gg \varepsilon$), $m^{(0)}=m_{ref}$, $v_k^{(0)} = v_k$ and $\Phi_d^{(n)} \gg 1.0$.

step 2: While ($\delta^{(n)} > \varepsilon$ and $\left|\Phi_d^{n+1} - 1.0\right| > 0.1$ and $i<C1$)

1: Update membership value, $u_{jk}^{(n+1)}$ based upon $m^{(n)}$ and $v_k^{(n)}$.

2: Update cluster center, $v_k^{(n+1)}$ based upon $m^{(n)}$, $u_{jk}^{(n+1)}$ and t_k.

3: The CG (Conjugate gradient algorithm) algorithm is used to obtain $m^{(n+1)}$ based on $u_{jk}^{(n+1)}$, $v_k^{(n+1)}$.

4: Compute the relative change in total objective function:

$$\delta^{(n+1)} = \frac{\left\|m^{(n)} - m^{(n+1)}\right\|_2^2}{\left\|m^{(n+1)}\right\|_2^2}.$$

5: According to equation 3, calculate data misfit $\Phi_d^{(n+1)}$. Then, compute $\Phi_d^{(n+1)} = \frac{\Phi_d^{(n+1)}}{N1}$, where $N1$ is target data misfit (The total number of gravity data.).

6: n=n+1, $i=i+1$.

End

step 3: According to Equation 3 and 17, calculate the data misfit and the variance of each cluster of the inversion result from step 2. Next, record those data to prepare for subsequent operations.

Go to the step 1, if the parameter pairs of λ and η are not used up.

3. The parameter values selected in step 1 and step 2 may not be optimal. Therefore, it is necessary to adjust their values and choose the most reasonable parameter values. Sequentially, the values of the three parameters β, λ, and η are adjusted based on the results of the previous two steps. In this parameter adjustment process, the terminal tolerance value ε is reduced while the number of iterations *C1* increases, still using Algorithm 1 for inversions. Consequently, the corresponding optimal values of each parameter set also produce tiny variance values of each cluster and the data misfit is close to the expected target data misfit.
4. Finally, perform the final inversion using the reference model obtained from step 1 and the most reasonable weighting parameters after the adjustment operation. Similarly, continue to use Algorithm 1 to reduce the termination tolerance value ε without limiting the number of iterations *C1* to ensure optimal inversion results. The details of the FCM inversion are described in Algorithm 3.

Algorithm 2 Automatic search algorithm for weighted parameter optimal values of λ and η

Compute reference model vector, m_{ref}, from smooth inversion. Initialize the initial clustering center v_k *(k=1,2)*. Determine the target values, t_k *(k=1,2),* based on a priori petrophysical data. Set i=1. Initialize $m^{(0)}=m_{ref}$, $v_0^{(1)}=v_1, v_0^{(2)}=v_2, \lambda^{(0)}$ and $\eta^{(0)}$. Set $v_1^{(1)}=v_1+\varepsilon, v_2^{(1)}=v_2-\varepsilon$ (ε is a small positive constant.).

step 1: Do While ($v_1^{(1)}>v_0^{(1)}$ or $v_2^{(1)}< v_0^{(2)}$)

Compute membership function values, $u_{jk}^{(0)}$ (j=1,2,3...N) based upon $m^{(0)}$, $v_0^{(1)}$, and $v_0^{(2)}$. N is the total number of meshing cells.

Compute cluster center, $v_k^{(0)}$ based upon $m^{(0)}$, $u_{jk}^{(0)}$, t_k and $\eta^{(i)}$.

Compute $m^{(1)}$, based upon $m^{(0)}$, $u_{jk}^{(0)}$, $v_k^{(0)}$, $\lambda^{(i-1)}$, $\eta^{(i-1)}$ and t_k.

Update membership function values, $u_{jk}^{(1)}$ (j=1,2,3...N) based upon $m^{(1)}$, , and $v_k^{(0)}$.

Update cluster center, $v_k^{(1)}$ based upon $m^{(1)}$, $u_{jk}^{(1)}$, t_k and $\eta^{(i)}$.

$i=i+1$;

$\lambda^{(i)}=\eta^{(i-1)}$;

$\eta^{(i)}=1.5\bullet\eta^{(i-1)}$;

End

step 2: $\lambda=\lambda^{(i-1)}$; $\eta=\eta^{(i-1)}$.

2.4. Analysis of Original and New Inversion Methods

To test the proposed method for discrete-valued gravity inversion, inversions are carried out using synthetic gravity data.

A depiction of the true model is shown in Fig. 1a. Obviously, we take $t_1 = 0.0$ g/cc and $t_2 = 1.0$ g/cc. The gravity anomaly values are calculated using a simple model contaminated with random Gaussian noise with zero mean and standard deviation of 0.2 gu. Figure 1b shows the distribution of the gravity anomaly. The surface data are calculated on a 100×100 m^2 grid, with 100 m spacing. The total number of computational points is 441.

Using these data, we illustrate the improvements in the recovered density contrast models obtained using the improved method. Firstly, we start by inverting the data without clustering and determine the initial optimal value of β. Figure 1c shows the results of using the L-curve method to obtain the optimal regularization weighting parameter, providing an optimal value of 251,188.703. Figure 1d shows the results of regularization inversion. The result exhibits lower density contrast values near the edges of the block and smaller petrophysical values compared with the true model.

Secondly, we conduct the original guided FCM clustering inversion. Using the value of β and the reference model recovered by the smooth inversion, we perform step 2 of the inversion workflow for clustering inversion to determine the set $\lambda - \eta$. Figure 2 shows the values of the data misfit (a) and the variance of each cluster (b, c). The value of λ is chosen to be 51, while the value of η is 10,000. When this pair of weighting parameters is selected, the inversion results show that the data misfit is 444, close to the total number of gravity data, while the variance of each cluster is small. Subsequently, we perform step 3 to obtain the optimal values of the three weighting parameters and conduct the final inversion. Figure 2d shows the result of the original inversion workflow.

Compared with the regularized inversion, the result of the original FCM clustering inversion is greatly improved. The spatial distribution of the petrophysical inversion model is closer to the real

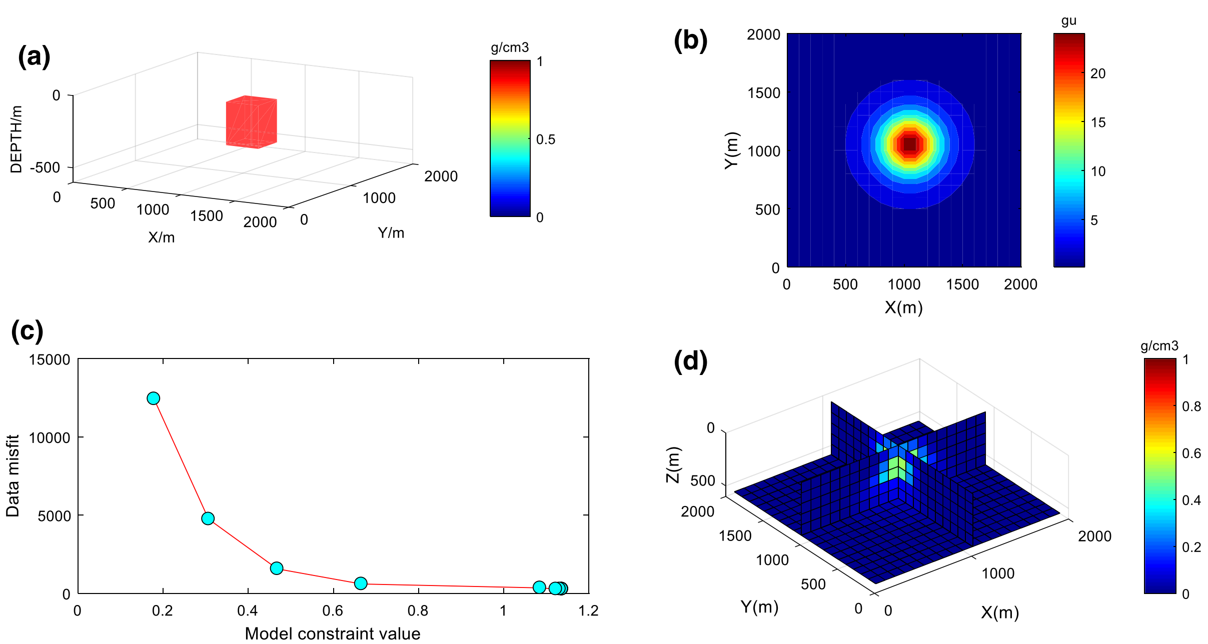

Figure 1
a Spatial location of a single model. **b** Contour map of forward gravity anomaly of single model with added Gaussian noise. **c** Determination of optimal regularization weighting parameters using the L-curve method. **d** Combined result slices of regularized inversion

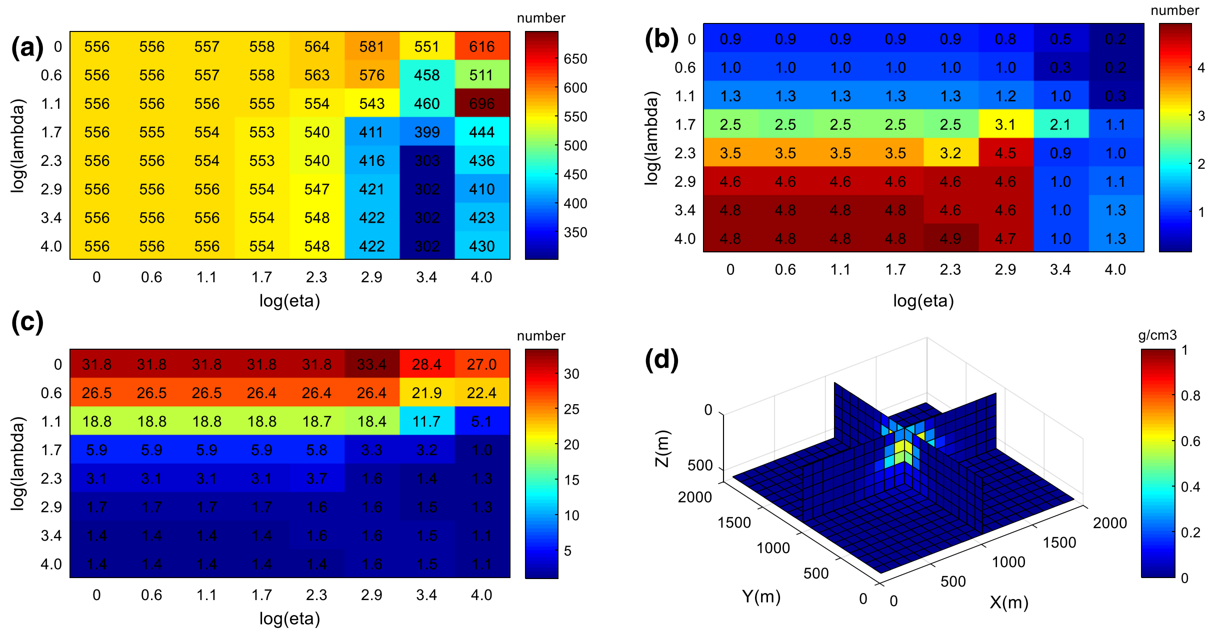

Figure 2

Original fuzzy *C*-means clustering inversion performed on the theoretical data of the simple model. **a** Values of the data misfit, **b**, **c** variance of each cluster using the original guided FCM clustering algorithm of a single model. **d** Combined result slices of the original FCM inversion

model, and the density values of the result are well gathered around the values of the prior property information. Compared with the regularized inversion results, the inversion results are significantly better, but a large gap with the actual model still remains.

Similarly, retaining the value of β and the reference model obtained in step 1, we perform steps 2 and 3 of the inversion workflow using the improved guided fuzzy clustering algorithm. Figure 3 shows the values of the data misfit (a) and the variance of each cluster (b, c) obtained from the improved guided FCM clustering inversion. The value of λ is chosen to be 10,000, while the value of η is 10,000. Also, the inversion results show that the data misfit is 408, close to the total number of gravity data, while the variance of each cluster is small. We then carry out step 3 to obtain the optimal values of the three weighting parameters and conduct the final inversion. Figure 3d shows the results of the original inversion workflow.

The results shown in Figs. 2 and 3 all show distinct boundaries between different geological features for the two types of clustering inversion, but the density values from the latter inversion are better gathered around the discrete prior property values. Comparing Figs. 2a–c with 3a–c, in terms of data selection of the same magnitude, there are obviously more pairs of parameters available for selection of the parameters *a* and *b* in Fig. 2. However, the wide choice of parameter pairs means that the algorithm is not sensitive to changes in the values of the weighted parameter pairs. When selecting a parameter pair from the perspective of numerical magnitude, the original algorithm is often confused and chooses a pair of nonoptimal weighted parameter pairs. However, the improved algorithm shows a very small area of selectable parameter values in Fig. 3a–c. When using the enumeration method for parameter pair selection, if the optimal parameter pair value lies outside the originally set parameter value range, it will be difficult to obtain optimized numerical parameters. It can be clearly seen by comparing Figs. 2a–c and 3a–c that the available weighted parameter pairs often have values of the parameter η greater than or equal to the values of the parameter λ.

We next analyze why there are more unusable weighted parameter pairs when using the new FCM inversion scheme. Initialize the initial cluster center

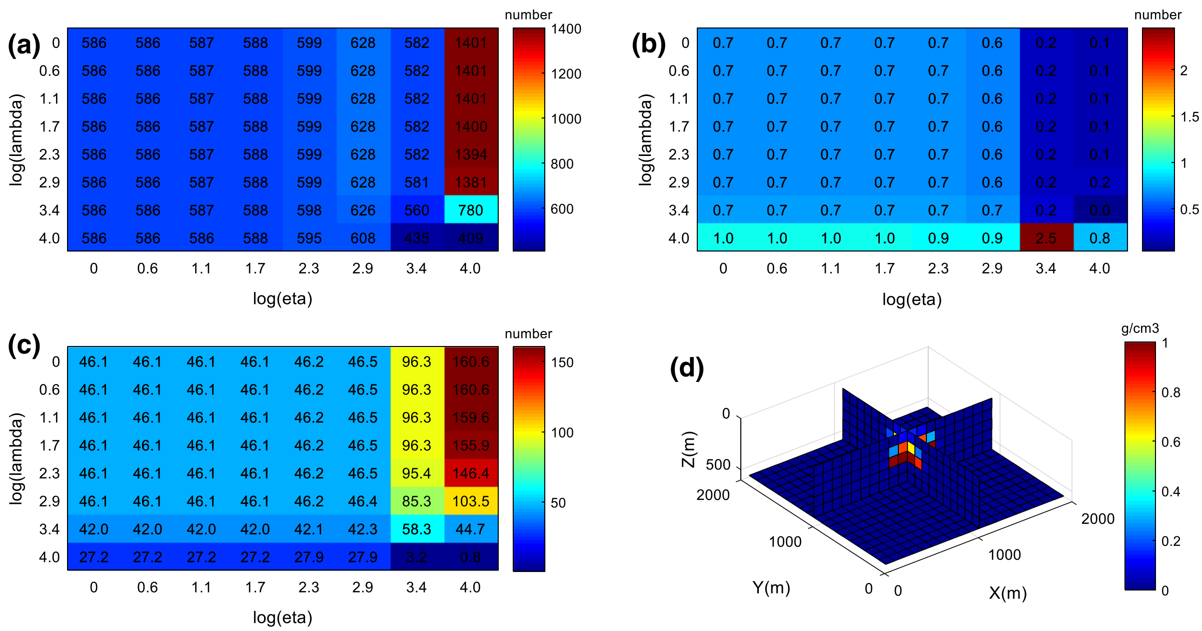

Figure 3
Improved fuzzy *C*-means clustering inversion performed on the theoretical data of the simple model. **a** Values of the data misfit, **b**, **c** variance of each cluster using the improved guided FCM clustering algorithm of a single model. **d** Combined result slices of the improved FCM inversion

values as $v_1 = 0.05$ g/cc and $v_2 = 0.20$ g/cc. Three pairs of weighted parameter values $(\lambda, \eta) = \{(100, 100), (500, 500), (2000, 2000)\}$ and Algorithm 3 are used to illustrate the difference between the original method and the improved method based on the reference model and regularization parameter β obtained from step 1 of the inversion workflow. Using $\lambda = 100$ and $\eta = 100$, the improved method yields the results shown in Fig. 4a while the original method yields those shown in Fig. 4b. It can be seen that the values of the cluster centers in Fig. 4a are gradually decreasing, while the values of the cluster centers in Fig. 4b are gradually increasing and approach the target cluster centers. Similarly, Fig. 4c, d $(\lambda, \eta) = \{(500, 500)\}$ and Fig. 4e, f $(\lambda, \eta) = \{(2000, 2000)\}$ show similar results. In the inversion process, the final aim of the parametric search is to find pairs of weighted parameters with small variances. It can be concluded that, when selecting an unreasonable weighted parameter pair, the cluster centers updated by the improved algorithm will exhibit a large variety of variance values, which ultimately renders the parameter pair unsuitable.

It can be seen from Fig. 4b, d, f that the cluster center values calculated based on the original FCM method algorithm are all changed with respect the target cluster centers, and the cluster centers change rapidly. As shown in Fig. 2a–d, the range of weighting parameters is large, often selecting nonoptimal parameter pairs. However, the values of the petrophysical model are updated more slowly to the petrophysical constraint information. When a better result is not achieved, the iteration ends. From Fig. 2a–d, the range of weighting parameters is chosen to be large, and nonoptimal weighted parameter pairs are often chosen. However, the values of the petrophysical property model are updated more slowly towards the petrophysical prior information, and the iteration ends when the inversion results have not yet been reached. Therefore, it becomes critical to design a search algorithm to obtain the two weighting parameters according to the guided cluster constraint.

2.5. *Weighted Parameter Search Algorithm*

Based on the above analysis, we propose a search algorithm from the new FCM clustering inversion

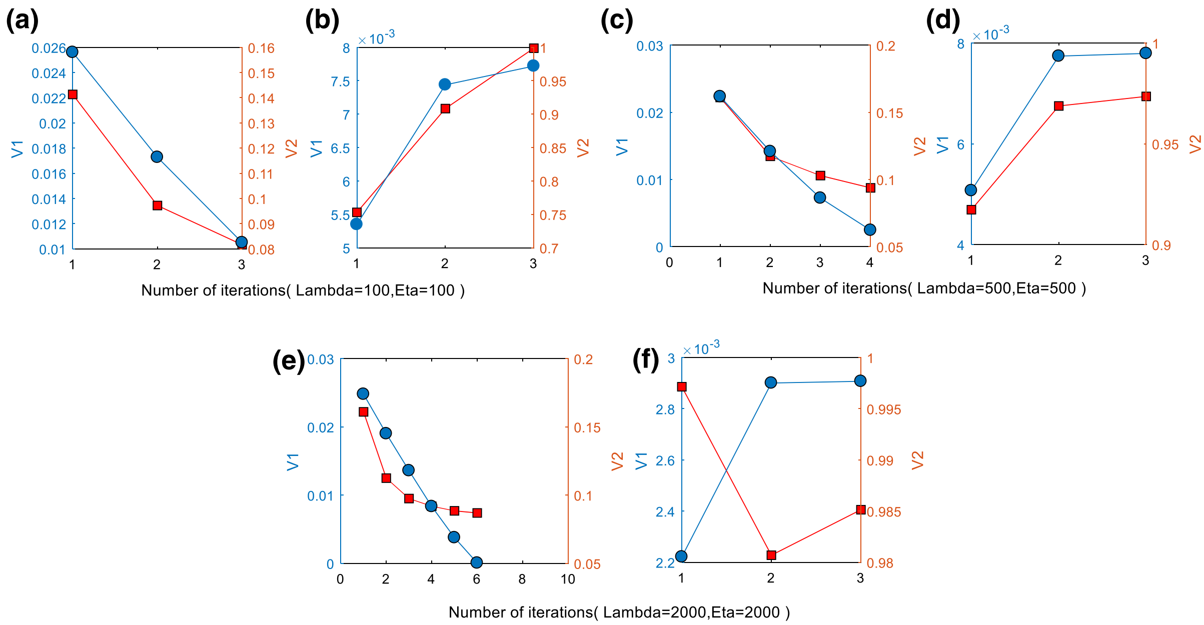

Figure 4

The changes (**a**, **c**, **e**) show in the clustering center during the implementation based on improved FCM inversion with different parameter set. The changes (**b**, **d**, **f**) present t is presented in the cluster center during the original FCM inversion using different weighting parameter pair. The red and blue lines show the changes in cluster centers v_1 and v_2, respectively

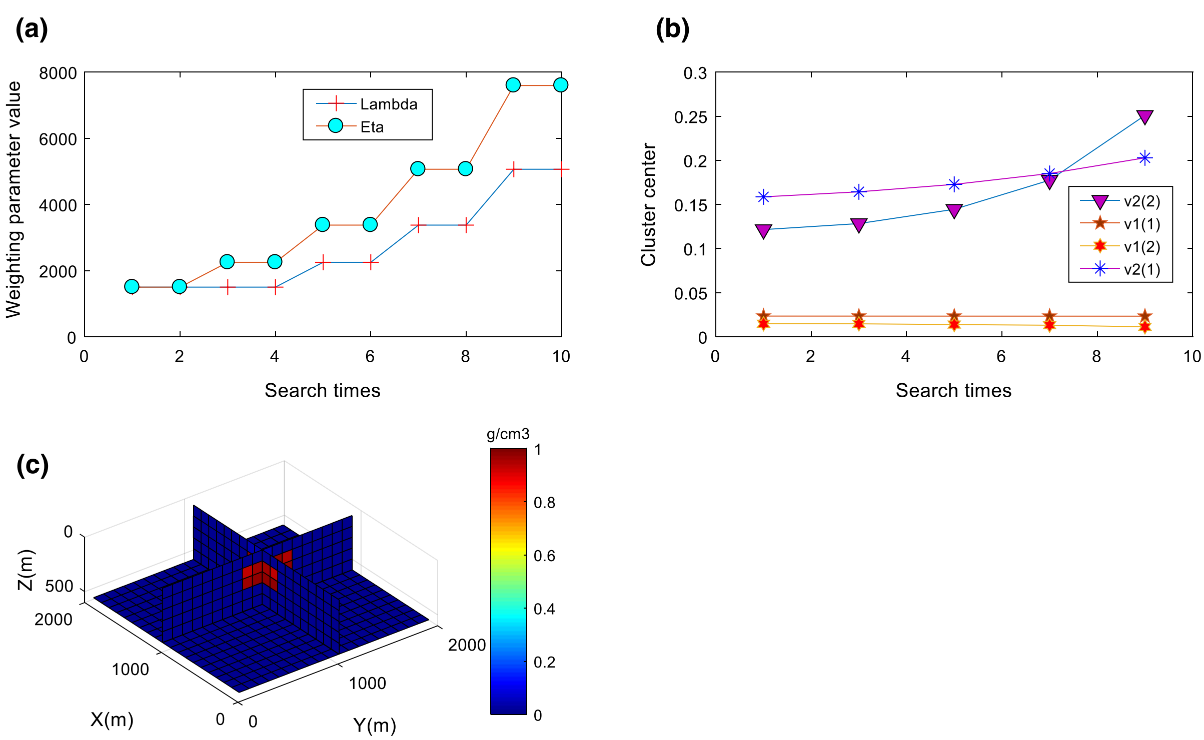

Figure 5

The process of automatically clustering weighted parameters to search for optimal values. The variation curve of the weighting parameters (**a**) and the two types of cluster center (**b**) values in the parameter search process. **c** Combined result slices of improved FCM inversion based on the optimized parameters from the search algorithm

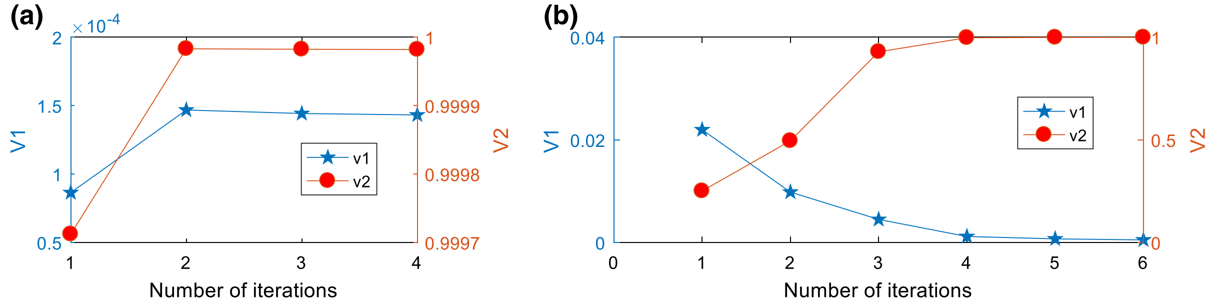

Figure 6
In the final inversion process, the numerical curves of the cluster centers of the simple model. The numerical change of the cluster centers in the iterative process of the final inversion using the original (**a**) and improved FCM inversion method (**b**)

scheme for optimal values of the weighting parameters $\lambda - \eta$. We can now formulate the problem of finding the optimal weighting parameters as follows: find (λ, η) such that the updated cluster centers are changed in the direction of the target cluster centers. In other words, the cluster centers obtained in the second calculation tend to be closer to the target cluster centers than the cluster centers obtained in the first time. Essential to the implementation of the searching algorithm, summarized in Algorithm 3, are four building steps. In step 1, the conjugate gradient method is used to obtain the petrophysical parameter values of the model.

This search algorithm relies on two criteria. The first is that the values of the updated cluster centers change to the target cluster centers, while the other is

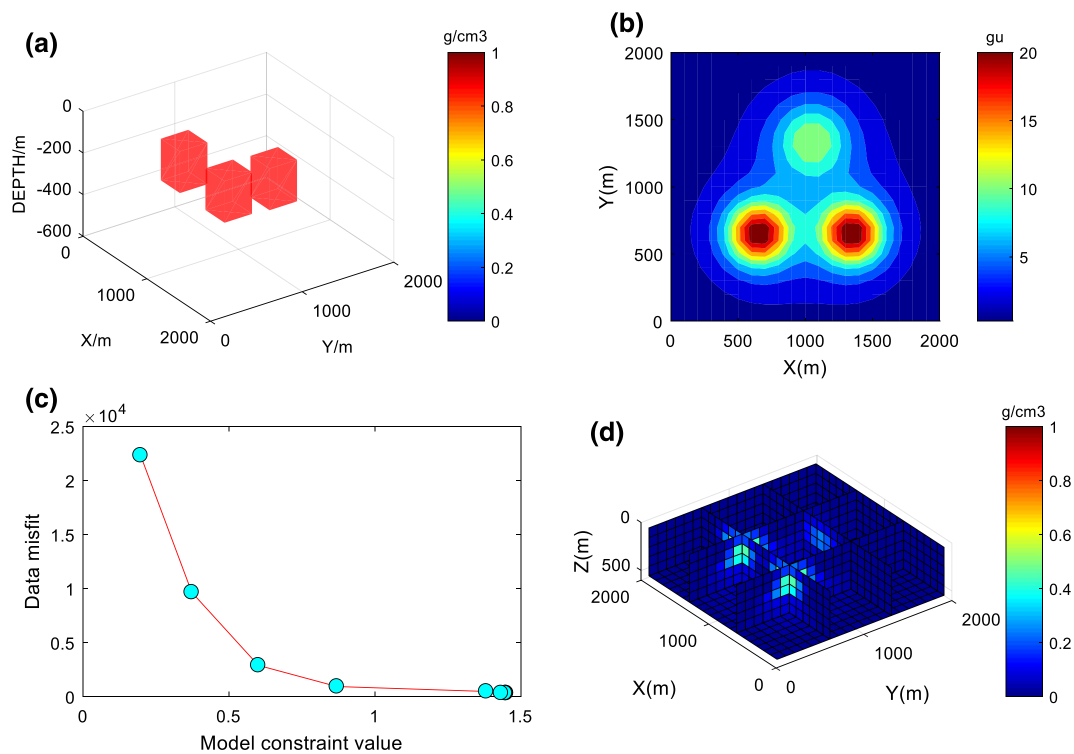

Figure 7
a Spatial location of model 2. **b** The contour map of forward gravity anomaly of the complicated model with added Gaussian noise. **c** Determination of the optimal regularization weighting parameters using the L-curve method. **d** Combined result slices of the regularized inversion

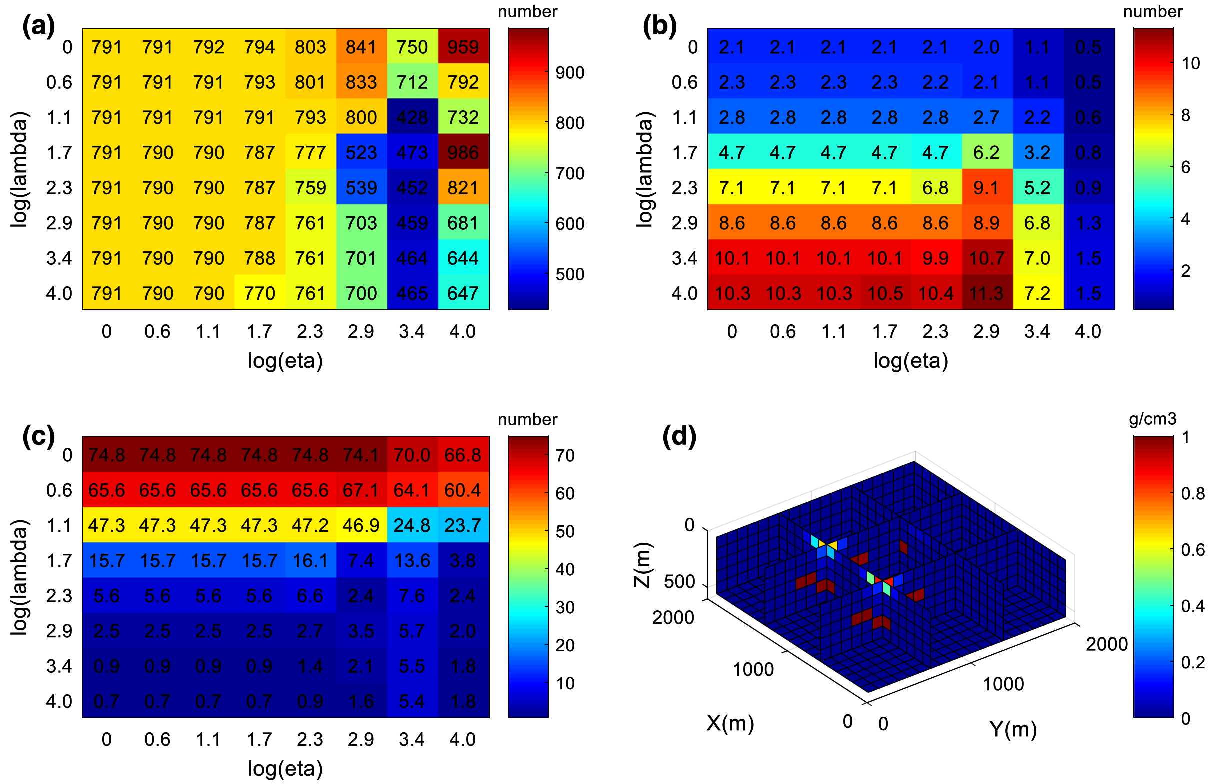

Figure 8

Original fuzzy C-means clustering inversion performed on the theoretical data of the simple model. **a** Values of the data misfit, **b**, **c** variance of each cluster using the original guided FCM clustering algorithm of a single model. **d** Combined result slices of original fuzzy C-means inversion

that the value of the parameter λ be less than or equal to the value of the parameter η. If the updated cluster centers are farther away from the target cluster centers than the cluster centers obtained the previous time, continue to adjust the parameter values of $\lambda - \eta$. Continue the above operations until a reasonable pair of weighted parameters are selected. The search algorithm is validated in the following sections.

3. *Results and Validation*

To test the proposed method for discrete-valued gravity inversion, we carry out several inversions using synthetic data.

3.1. *Simple Model Test*

We use the above data to verify the search algorithm, applying the reference model and the regularization weighting parameter obtained from the above operations. The values of the initial cluster centers are set to $v_1 = 0.05$ g/cc and $v_2 = 0.20$ g/cc and the initial values of λ and η to 1500.

Figure 5a shows the changes in the values of the weighting parameters λ and η throughout the parameter search process. Figure 5b illustrates the changes of the two types of cluster centers. In Fig. 5b, v1(1) and v1(2) represent the values of the first cluster center calculated in the first and second time, respectively, while v2(1) and v2(2) represent the values of the second cluster center obtained by the first and second calculations, respectively. The weighted parameter pairs are transformed five times, yielding ten results. We find that the value of the first cluster center from the second calculation is always

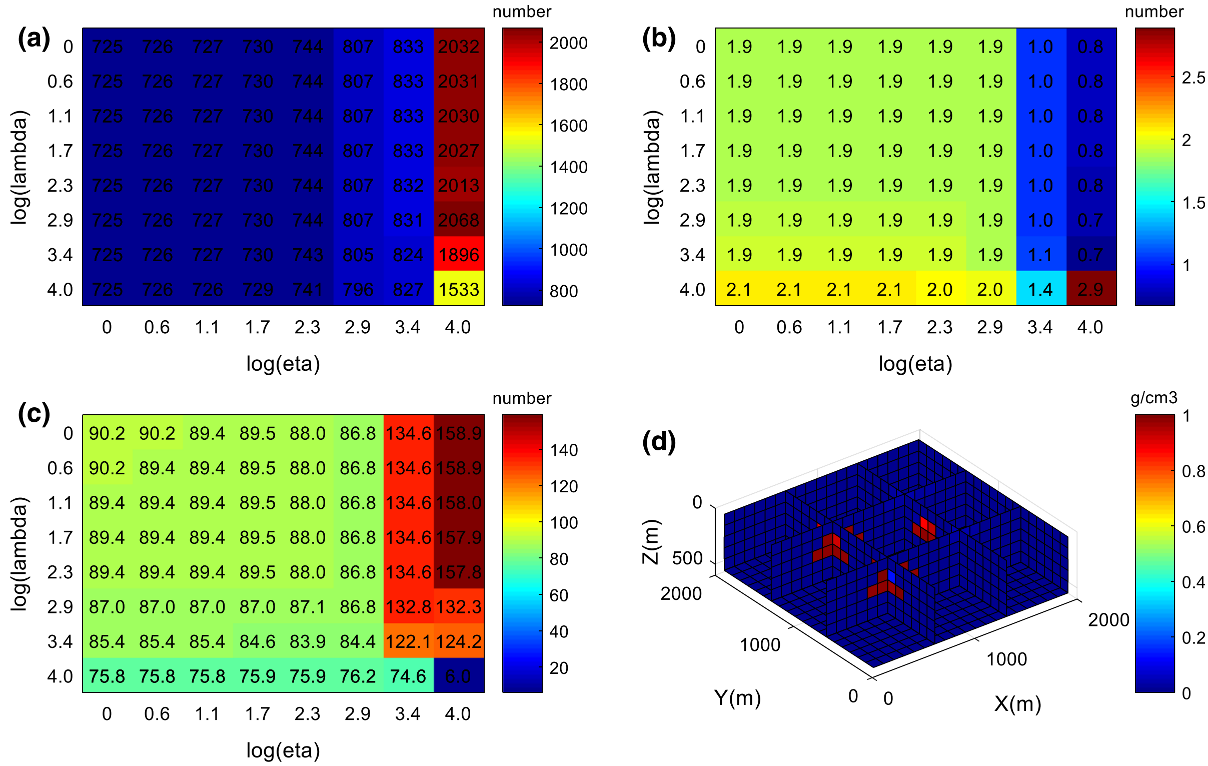

Figure 9
Original fuzzy *C*-means clustering inversion performed on the theoretical data of a complicated model. **a** Values of the data misfit, **b**, **c** variance of each cluster using the original guided FCM clustering algorithm of the complicated model. **d** Combined result slices of original FCM inversion

smaller than the corresponding value that computed from the first calculation. However, until the last time, the values of the clustering weighted parameter pair change, and the second clustering center obtained from the second calculation is larger than the value obtained from the first calculation. Ultimately, one gets λ equal to 5062.5 and η equal to 7593.75.

We replace the parameter pair obtained in the second step of the inversion workflow using the last transformed parameter pair in the calculation process of the search algorithm. Then, consistent with the inversion workflow, the values of the weighting parameters β, λ, and η are adjusted separately to obtain the optimal values of the three weighting parameters. Finally, performance of step 4 in the inversion workflow yields the results shown in Fig. 5c. Comparison of Figs. 5c, 1d, 2d and Figs. 3d, 5c reveals a better inversion result. Not only are the boundaries between different anomalies more obvious, but the values of the inversion results are better clustered around the two types of petrophysical constraint information. Moreover, the parameter search only requires ten times, which greatly improves the search speed compared with the number of calculations required for the enumeration method for the parameter search. This example verifies the correctness of the algorithm. Using the inversion workflow, Fig. 6a or b shows the cluster center changes of the original or improved FCM inversion method. From Fig. 1d, the petrophysical properties of the reference model are mostly concentrated around 0.0 g/cc and 0.15 g/cc. Comparing Fig. 6a and b, it is found that, when the original FCM method is used for inversion, the cluster centers are updated very quickly, and the target cluster center are approached in just a few steps. However, the improvement scheme shows that the cluster centers change

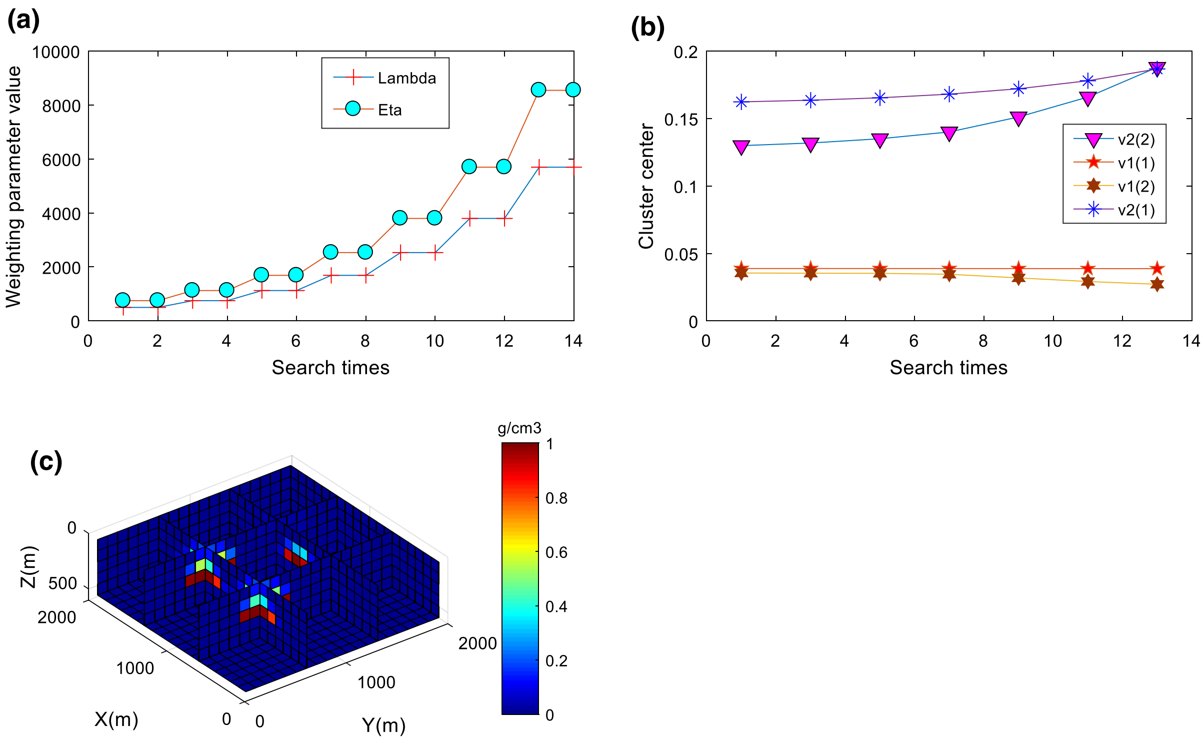

Figure 10
The process of automatically clustering weighted parameters to search for optimal values. The variation curve of the weighting parameters (**a**) and the two types of cluster centers (**b**) in the parameter search process. **c** Combined result slices of the improved FCM inversion based on the optimized parameters from the search algorithm

gradually, which is undoubtedly more consistent with the trend of the density variation of the model. The clustering centers always explain the distribution characteristics of the data to some extent. Obviously, the cluster centers obtained by using the new method can better explain the actual distribution characteristics of the petrophysical model data, so it can be considered that the calculated cluster centers are more reasonable.

Next, we use more complex examples to verify the correctness of the proposed algorithm.

3.2. Model Test 2

Model 2 is depicted in Fig. 7a. Figure 7b shows the gravity anomaly values contaminated with random Gaussian noise with zero mean and standard deviation of 0.2 gu. The surface data are also calculated on a $100 \times 100\ m^2$ grid, with 100 m spacing.

Firstly, we carry out the regularization inversion and determine the value of β. Figure 7c displays the results of the L-curve method to obtain the optimal regularization weighting parameter, 251,188.703. Figure 7d shows the results of the regularization inversion. The results show lower density contrast values near the edges of the block and smaller petrophysical values compared with the true model.

Then, we execute the operations of the inversion workflow using the original FCM method. Similarly, an initial set of $\lambda - \eta$ in step 2 of the inversion workflow is determined. Figure 8 shows the values of the data misfit (a) and the variance of each cluster (b, c). The values of λ and η are both chosen to be 10,000, while the corresponding data misfit is 647, and the variance values of the two classes are all small. We perform step 3 in the inversion workflow to obtain the optimal values of the three weighting parameters and carry out the final inversion. Figure 8d shows the results obtained from the original FCM inversion.

Then, retaining the value of β and the reference model, we perform step 2 of the inversion workflow using the improved FCM algorithm. Figure 9 shows the values of the data misfit (a) and the variance of each cluster (b, c). The values of λ and η are also both chosen to be 10,000. At this point, only a better combination is selected from bunches of parameter pairs, but this parameter pair results in a larger variance value and data misfit. Next, carry out step 3 to adjust the three weighting parameters and conduct the final inversion. Figure 9d shows the results obtained from the improved FCM inversion using the inversion workflow.

Next, the gravity data of model 2 are used to prove the correctness of the weighted parameter search algorithm of Algorithm 2. Use the reference model and the β, set values of the initial cluster centers of v_1 = 0.05 g/cc and v_2 = 0.20 g/cc, make the initial values of λ and η both equal to 1500, and perform the parameter search algorithm. Figure 10a displays the changes in the values of λ and η throughout the parameter search process. Figure 10b shows the changes in the values of the two cluster centers. The weighted parameter pairs are transformed for 7 times, yielding 14 results. In this example, λ equals 5695.31 and η equals 8542.97.

Algorithm 3 Iterative algorithm for FCM inversion

Initialize regularization parameter, β from L-curve method. Compute reference model vector, m_{ref}, from smooth inversion. Assign termination tolerance value ε (a smaller positive constant, 5E-2). Initialize the initial clustering center v_k *(k=1,2)*. Based on available a priori petrophysical data, determine the target values, t_k *(k=1,2)*. Initialize the set of parameter pairs for λ and η from carried out searching algorithm.

step 1: Set i=0 and n=0. Initialize $\delta^{(0)}(\delta^{(0)} \gg \varepsilon)$, $m^{(0)}=m_{ref}$, $v_k^{(0)} = v_k$ and $\Phi_d^{(n)} \gg 1.0$.

step 2: While ($\delta^{(n)} > \varepsilon$ and $\left|\Phi_d^{n+1} - 1.0\right| > 0.1$)

1: Update membership value, $u_{jk}^{(n+1)}$ based upon $m^{(n)}$ and $v_k^{(n)}$.

2: Update cluster center, $v_k^{(n+1)}$ based upon $m^{(n)}$, $u_{jk}^{(n+1)}$ and t_k.

3: The CG (Conjugate gradient algorithm) algorithm is used to obtain $m^{(n+1)}$ based on $u_{jk}^{(n+1)}$, $v_k^{(n+1)}$.

4: Compute the relative change in total objective function:

$$\delta^{(n+1)} = \frac{\left\|m^{(n)} - m^{(n+1)}\right\|_2^2}{\left\|m^{(n+1)}\right\|_2^2}.$$

5: According to equation 3, calculate data misfit $\Phi_d^{(n+1)}$. Then, compute

$$\Phi_d^{(n+1)} = \frac{\Phi_d^{(n+1)}}{N1}$$, where $N1$ is target data misfit.

6: n=n+1, i=i+1.

End

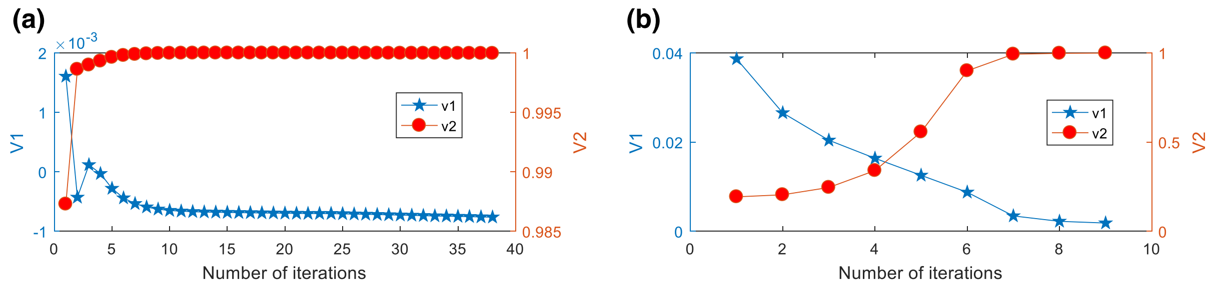

Figure 11
In the final inversion process, the numerical curves of the cluster centers of the second model. The numerical change of cluster centers in the iterative process of the final inversion using the original (**a**) and improved FCM inversion method (**b**)

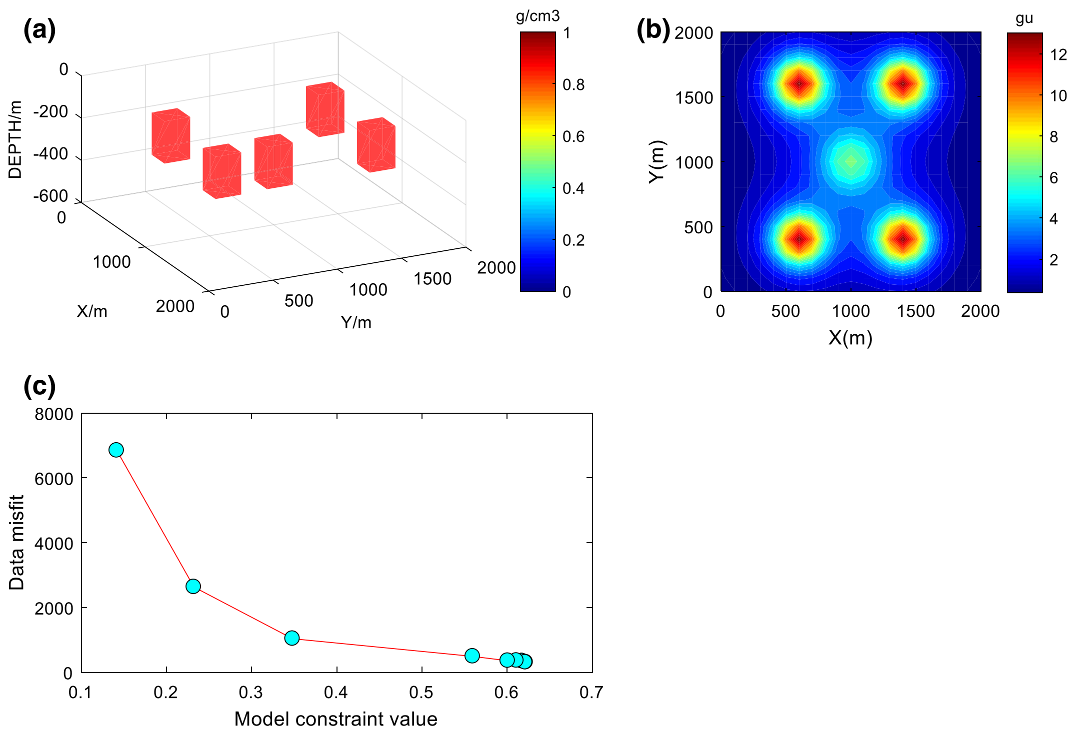

Figure 12
a Spatial location of model 3. **b** Contour map of forward gravity anomaly of complicated model with added Gaussian noise. **c** Determination of optimal regularization weighting parameters using the L-curve method

Then, we use the parameter pair obtained from the parameter search algorithm and adjust the values of the weighting parameters β, λ, and η separately. Finally, the final inversion is performed, yielding the results shown in Fig. 10c based on the adjusted weighting parameters. Comparing Figs. 8d, 10c, and Figs. 9d, 10c reveals more obvious boundaries between different blocks, and the values of the inversion result are better clustered around the prior petrophysical information. Moreover, the parameters search only needs 14 times, which also improves the speed of the parameter search process. Figure 11a and b show the changes in the values of the cluster centers when using the original or improved FCM inversion. Comparing Fig. 11a and b, it is found that the cluster centers are updated very quickly, and the target cluster centers are also approached in just a few steps when using the original FCM method for

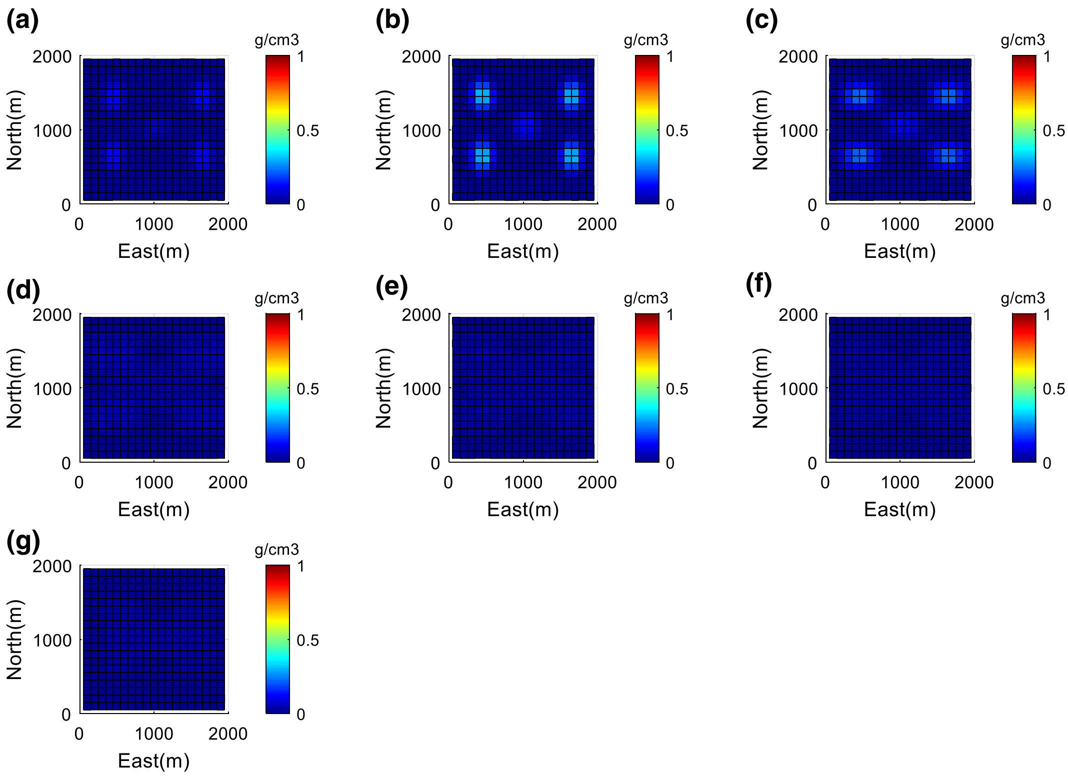

Figure 13
Regularized inversion of the test of model 3, and the stratified results of the inversion at z equals 50 m (**a**), 150 m (**b**), 250 m (**c**), 350 m (**d**), 450 m (**e**), 550 m (**f**), and 650 m (**g**)

inversion. However, the cluster centers change gradually when using the improved FCM inversion method. Obviously, the cluster centers obtained using the new method can better explain the actual distribution characteristics of the petrophysical model, thus it can also be considered that the calculated cluster centers are more reasonable.

3.3. Model Test 3

The third model is used to test the algorithm. A depiction of the true model is shown in Fig. 12a. The gravity anomaly of model 3 contaminated with random Gaussian noise with zero mean and standard deviation of 0.2 gu is shown in Fig. 12b. We retain the same number of data points and the same dot and line spacing as in the above two models.

Firstly, we perform the regularization inversion and determine the value of β. Figure 12c shows the results of using the L-curve method, yielding an optimal value of the regularization parameter of 251,188.0. Figure 13a–g shows the inversion results for each layer at different depth. The inversion results are similar to the above examples. The results show lower density contrast values near the edges of the blocks and smaller densities compared with the true model.

Then, we perform the inversion workflow using the original FCM method. Figure 14 shows the values of the data misfit (a) and the variance of each cluster (b, c). The values of λ and η are chosen to be 794 or 10,000. The corresponding data misfit is 647, and the variance values are small. Then, the values of the three weighting parameters are adjusted and the final inversion is carried out. Figure 15 displays the inversion results for each layer at different depth.

In this model test, we directly use the parameter search algorithm to prove the advantages of the proposed algorithm. Continue to use the reference model and the regularization parameter obtained from

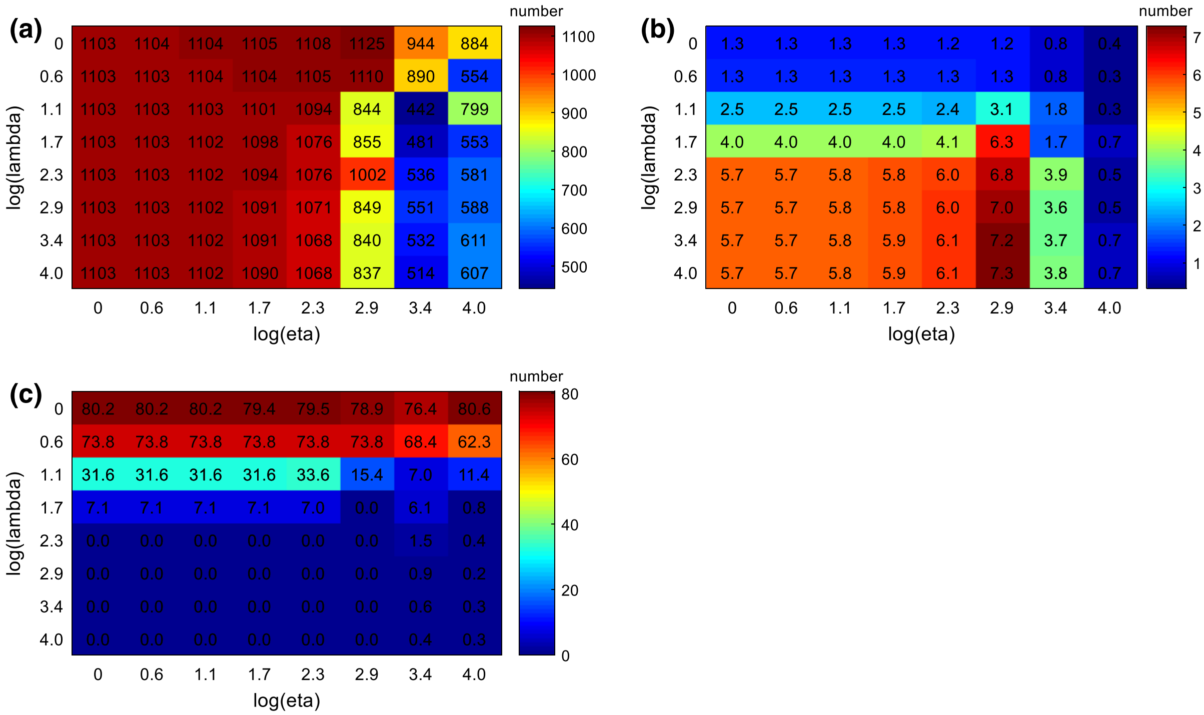

Figure 14
Original fuzzy *C*-means clustering inversion performed on the theoretical data of model 3. **a** Values of the data misfit, **b**, **c** variance of each cluster using original guided FCM clustering algorithm of complicated model

step 1 in the inversion workflow. The initial values of the cluster centers are set to $v_1 = 0.05$ g/cc and $v_2 = 0.20$ g/cc and the initial values of λ and η to 1500 and then we perform the parameter search algorithm; Fig. 16a shows the changes in the values of λ and η throughout the parameter search process. Figure 16b displays the variation of the cluster centers in this process. The weighted parameter pairs are transformed for 12 times, yielding λ of 7593.75 and η of 11,390.6250.

Then, use the parameter pair obtained from the parameter search algorithm of model 3 and adjust the values of β, λ, and η separately. Finally, the final inversion is performed using the improved FCM method to obtain the results shown in Fig. 17. Comparing Figs. 15, 17, and Figs. 13, 17 reveals clearer boundaries between different blocks and more clustered results around the two discrete petrophysical constraints. Moreover, the parameter search algorithm accelerates the speed of determining optimal and reasonable weighting parameters. Figure 18a, b shows the changes in the values of the cluster centers of the original and improved FCM inversion methods. Obviously, the cluster centers obtained using the new method can better explain the actual distribution characteristics of the petrophysical model. This example thus verifies the superiority of the proposed algorithm.

4. Conclusions

A new scheme for FCM inversion based on discrete petrophysical constraint information is proposed. The purpose of the method is to fully consider the data distribution characteristics of the model parameters in the inversion process and thereby obtain more reasonable cluster center values. Firstly, the theoretical data of a simple model and the methods in the inversion workflow are applied to verify the new FCM inversion method, revealing the following characteristics: (1) When using the

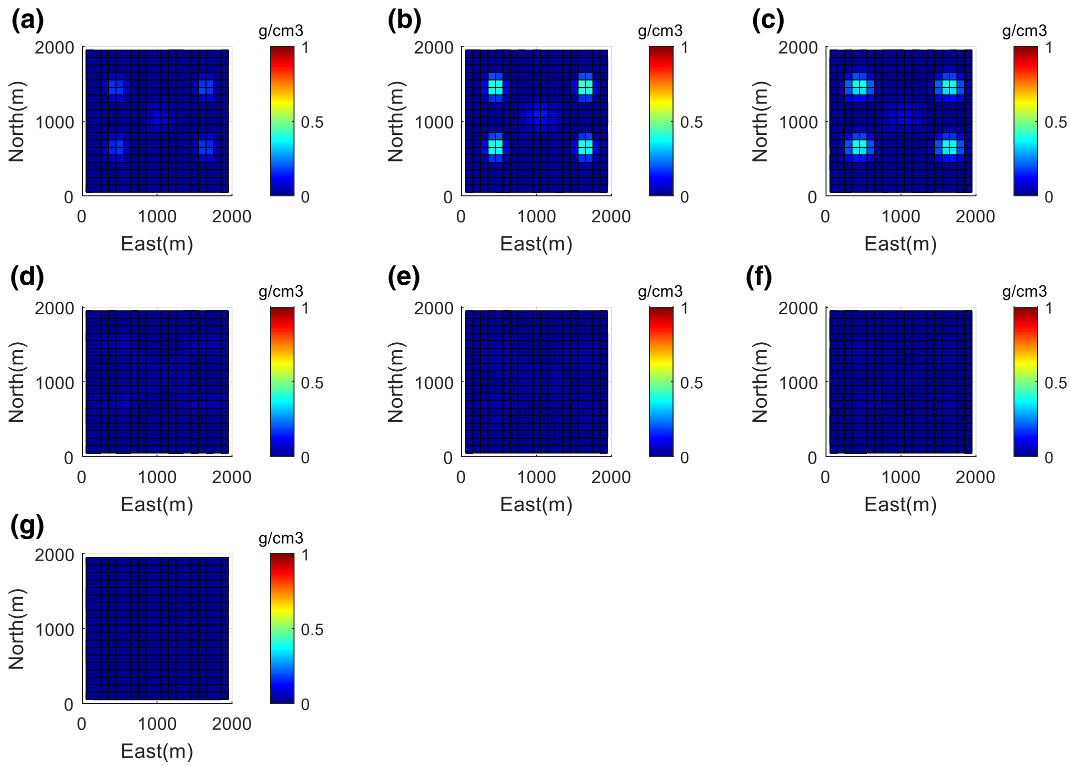

Figure 15
Original FCM inversion of the test of model 3, and the stratified results of the inversion at z equals 50 m (**a**), 150 m (**b**), 250 m (**c**), 350 m (**d**), 450 m (**e**), 550 m (**f**), and 650 m (**g**)

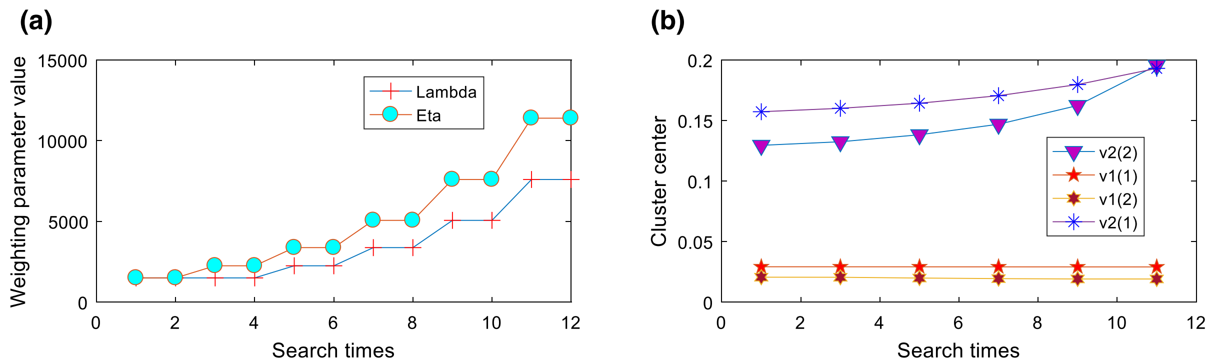

Figure 16
Process of automatically clustering weighted parameters to search optimal values of model 3 with the variation curve of the weighting parameters (**a**) and the two types of cluster centers (**b**) values in the parameter search process

enumeration method for the parameter search, the new inversion method is more sensitive to the weighted parameter values than the original inversion method. It appears that the weighting parameters have the same domain, while the original method has a wider range of applicable parameter values. However, the original method often selects a pair of nonoptimal weighting parameters due to the data representation in the parameter search process, leading to poor inversion results; (2) We use three sets of

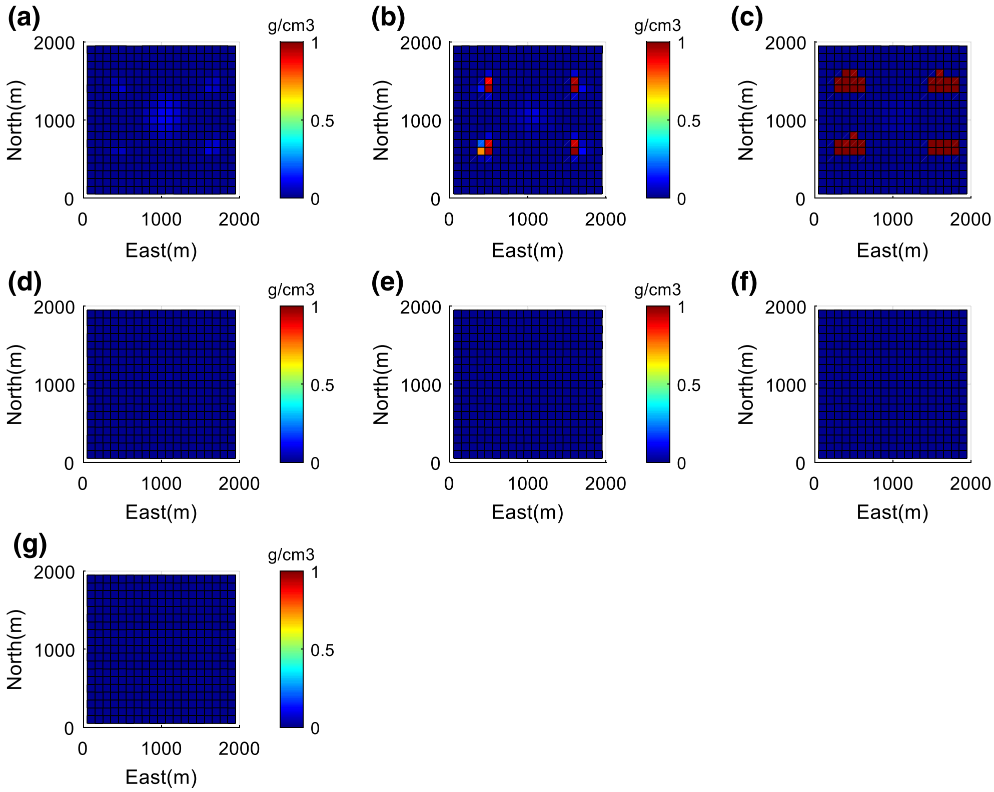

Figure 17
Improved FCM inversion performed using the weighted parameters obtained by the parameter search algorithm, and the stratified results of the inversion at z equals 50 m (**a**), 150 m (**b**), 250 m (**c**), 350 m (**d**), 450 m (**e**), 550 m (**f**), and 650 m (**g**)

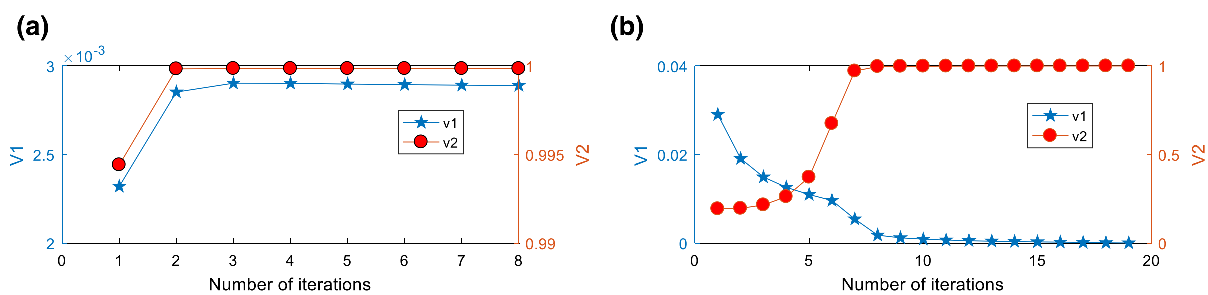

Figure 18
The numerical curves of the cluster centers of the test of model 3 in the iterative process of the final inversion using the original (**a**) and improved inversion method (**b**)

weighting parameters with different values to illustrate the difference between the original inversion method and the improved inversion means. The results show that the cluster centers calculated using the original FCM method always approach the target cluster centers, but the cluster centers calculated by the latter scheme show the opposite results. The basis for selecting the weighting parameters is that the obtained weighting parameter pairs must yield small variances between the two types of petrophysical parameter values and the target clustering centers. However, the improved FCM inversion scheme often leads to the opposite result. Therefore, we propose a parameter search algorithm for reasonable selection of the weighted parameter pairs in the improved inversion scheme.

We establish the following rules for the search algorithm: (1) the results of the parameter selection using the enumeration method reveal that the reasonable parameter pairs all have λ less than or equal to η. Therefore, in the parameter search algorithm, the parameter η is always maintained at 1.5 times the value of the parameter λ. (2) After transforming the weighting parameters, if the cluster centers obtained from the second computation tend towards the target cluster centers more than those calculated from the first calculation, an optimal weighting parameter pair has been selected.

Theoretical gravity data are used to verify the improved FCM method and the parameter search algorithm. Firstly, applying the operations mentioned in the inversion workflow to implement the new discrete-valued inversion method, we compare the results of the two clustering inversion using synthetic examples. The results show that the use of the improved method in the gravity inversion can increase the accuracy of the recovered results in terms of the definition of the boundaries and the petrophysical property values. Secondly, the theoretical gravity data are furthermore used to verify the parameter search algorithm based on the improved FCM inversion method. The results show that the parameter search algorithm can obtain optimal weighted parameters within a shorter number of computations. Using it to replace the weighted parameters obtained in the second step of the inversion workflow yields better final inversion results than the original FCM inversion method. Therefore, the new method and the new algorithm proposed herein are more efficient for geophysical inversion.

Acknowledgements

This work was supported by the National Key Research and Development Program of China Project (Grant No. 2018YFC0603502). We would like to thank Bing Zhang and Minao Sun for helpful discussions.

Publisher's Note Springer Nature remains neutral with regard to jurisdictional claims in published maps and institutional affiliations.

References

Aster, R. C., Borchers, B., & Thurber, C. H. (2016). *Parameter estimation and inverse problems* (2nd ed.). Cambridge: Academic. **(Paperback reprint of hardcover 2nd ed., 2011 edition ed.)**.

Camacho, A., Montesinos, F., & Vieira, R. (2000). Gravity inversion by means of growing bodies. *Geophysics, 65,* 95–101.

Chaovalitwongse, W., Androulakis, I. P., & Pardalos., P. M. (2008). Quadratic integer programming: complexity and equivalent forms. In C. A. Floudas & P. M. Pardalos (Eds.), *Encyclopedia of optimization* (pp. 3153–3159). US: Springer.

Constable, S. C., Parker, R., & Constable, C. G. (1987). Occam's inversion: a practical algorithm for generating smooth models from electromagnetic sounding data. *Geophysics, 52,* 289–300. https://doi.org/10.1190/1.1442303.

De Groot-Hedlin, C., & Constable, S. (1990). Occam's inversion to generate smooth, two dimensional models from magnetotelluric data. *Geophysics, 55,* 1613–1624.

Farquharson, C. G., Ash, M. R., & Miller, H. G. (2008). Geologically constrained gravity inversion for the Voisey's Bay Ovoid deposit. *The Leading Edge, 27,* 64–69.

Holtham, E., & Oldenburg, D. W. (2012). Large-scale inversion of ZTEM data. *Geophysics, 77*(4), WB37–WB45.

Krahenbuhl, R. A., & Li, Y. (2006). Inversion of gravity data using a binary formulation. *Geophysical Journal International, 167,* 543–556.

Krahenbuhl, R., & Li, Y. (2009). Hybrid optimization for lithologic inversion and time-lapse monitoring using a binary formulation. *Geophysics*, *74*, I55–I65.

Lane, R., FitzGerald, D., Guillen, A., Seikel, R., & McInerey, P. (2007). Lithologically constrained inversion of magnetic and gravity data sets. *ASEG Preview, 129,* 11–17.

Lelièvre, Peter G., & Oldenburg, D. W. (2009). A comprehensive study of including structural information in geophysical inversions. *Geophysical Journal International, 178,* 623–637.

Li, Y., & Oldenburg, D. W. (1996). 3D inversion of magnetic data. *Geophysics, 61,* 394–408. https://doi.org/10.1190/1.1443968.

Li, Y., & Oldenburg, D. W. (1998). 3D inversion of gravity data. *Geophysics, 63,* 109–119.

Li, Y., & Oldenburg, D. W. (2000). Joint inversion of surface and three component borehole magnetic data. *Geophysics, 65,* 540–552. https://doi.org/10.1190/1.1444749.

Li, Y., & Oldenburg, D. W. (2003). Fast inversion of large-scale magnetic data using wavelet transforms and a logarithmic barrier method. *Geophysical Journal International, 152,* 251–265.

Li, Z. G., Pan, F., & Lim, K. P. (2003). Adaptive basic unit layer rate-control for JVT: the 7th JVT meeting, Pattaya II JVT-G012-rl Thailand.

Li, Z. G., Pan, F., & Lim, K. P. (2004). Adaptive rate control for H. 264: Proc of IEEE Int Conf Image Process, pp. 745–748.

Li, Y., & Sun, J. (2016). 3d magnetization inversion using fuzzy c-means clustering with application to geology differentiation. *Geophysics, 81,* J61–J78.

Lin, Z., Wang, S., & Deng, Z. (2009). Generalization of FCM clustering algorithm for improved fuzzy partitioning research. *Computer Research and Development, 46,* 814–822.

Maag, Elizabeth, & Li, Y. (2018). Discrete-valued gravity inversion using the guided fuzzy c-means clustering technique. *Geophysics, 83,* G59–G77. **(IDGEO-2017-0594.R1)**.

Mackie, R. L., & Madden, T. R. (1993). Three-dimensional magnetotelluric inversion using conjugate gradients. *Geophysical Journal International, 115,* 215–229.

Newman, G. A., & Alumbaugh, D. L. (2000). Three-dimensional magnetotelluric inversion using non-linear conjugate gradients. *Geophysical Journal International, 140,* 410–424.

Parker, R. L. (1994). *Geophysical inverse theory*. NJ: Princeton University Press.

Phillips, N. D. (2001). Geophysical inversion in an integrated exploration program: examples from the San Nicolas deposit. M.Phil. thesis, University of British Columbia.

Sun, J., & Li., Y. (2010). Adaptive L-p inversion to recover both blocky and smooth features, in SEG technical program expanded abstracts 2010: Society of Exploration Geophysicists, SEG Technical Program Expanded Abstracts, pp. 4297–4301.

Sun, J., & Li, Y. (2015). Multidomain petrophysical constrained inversion and geology differentiation using guided fuzzy c-means clustering. *Geophysics, 80,* ID1–ID18.

Sun, J., & Li, Y. (2016). Joint inversion of multiple geophysical data using guided fuzzy c-means clustering. *Geophysics, 81,* ID37–ID57.

Uieda, L., & Barbosa., V. (2011). 3d gravity inversion by planting anomalous densities. In 12th International Congress of the Brazilian Geophysical Society & EXPOGEF, Rio de Janeiro, Brazil, 15–18 August 2011: Brazilian Geophysical Society, SEG Global Meeting Abstracts, pp. 867–871.

Williams, N. C. (2008). Geologically-constrained UBC-GIF gravity and magnetic inversions with examples from the Agnew-Wiluna Greenstone Belt, Western Australia. Ph.D. thesis, University of British Columbia.

Xing, T., Xing, Z., & Wan, F. (2010). FCM clustering algorithm based on information entropy. *Computer Engineering and Design, 23,* 5092–5095.

Zelt, C. A., & Barton, P. J. (1998). Three-dimensional seismic refraction tomography: a comparison of two methods applied to data from the Faeroe Basin. *Journal of Geophysical Research, 103,* 7187–7210.

Zhang, J. S., & Leung, Y. W. (2004). Improved possibilistic c-means clustering algorithms. *IEEE Transactions on Fuzzy Systems, 12*(2), 209–217.

(Received March 14, 2019, revised July 11, 2019, accepted August 14, 2019, Published online September 9, 2019)